

000 001 002 003 004 005 006 007 008 009 010 011 012 013 014 015 016 017 018 019 020 021 022 023 024 025 026 027 028 029 030 031 032 033 034 035 036 037 038 039 040 041 042 043 044 045 046 047 048 049 050 051 052 053 TALK2ME: HIGH-FIDELITY AND CONTROLLABLE AUDIO-DRIVEN AVATARS WITH GAUSSIAN SPLAT- TING

006
007 **Anonymous authors**
008 Paper under double-blind review

010 011 ABSTRACT 012

013 Audio-driven avatars are increasingly employed in online meetings, virtual hu-
014 mans, gaming, and film production. However, existing approaches suffer from
015 technical limitations, including low visual fidelity (e.g., facial collapse, detail loss)
016 and limited controllability in expression and motion, such as inaccurate lip syn-
017 chronization and unnatural head motion. Besides, most existing methods lack
018 explicit modeling of the correlation between facial expressions and head pose
019 dynamics, which compromises realism. To address these challenges, we pro-
020 pose Talk2Me, a high-fidelity, expressive, and controllable audio-driven frame-
021 work comprising three core modules. Firstly, we enhance 3D Gaussian Splat-
022 ting (3DGS) with Learnable Positional Encoding (LPE) and a modified Region-
023 Weighted Mechanism to mitigate facial collapse and preserve fine details. Sec-
024 ondly, an Expression Generator (EG) with an Audio-Expression Temporal Fusion
025 (AETF) module models the temporal relationship between audio and expression
026 features, enabling accurate lip-sync and natural expression transitions. Thirdly, a
027 Retrieval-Based Pose Generator (RBPG) explicitly captures the coupling between
028 expressions and pose dynamics, with a Pose Refiner (PR) enhancing the natural-
029 ness and continuity of head motion. We further construct a Mandarin monocular
030 video dataset featuring diverse identities to evaluate cross-lingual generalization.
031 Experiments demonstrate that Talk2Me outperforms state-of-the-art methods in
032 visual quality, synchronization accuracy, and motion naturalness.

034 035 1 INTRODUCTION 036

037 Audio-driven talking avatars have received increasing attention from both academia and industry.
038 This task involves cross-modal synthesis, where visual facial animations must be temporally aligned
039 with input audio. Such audio-driven avatars show strong potential in applications like virtual con-
040 ferencing, gaming, and film production (Li et al., 2023; Peng et al., 2023; Cho et al., 2024; Peng
041 et al., 2024). By bridging human interaction and digital media, this technology plays a central role
042 in immersive experiences and intelligent agents.

043 Despite recent advances, audio-driven avatar generation continues to face two fundamental chal-
044 lenges: achieving high visual fidelity and ensuring controllable facial and head dynamics. Methods
045 based on Generative Adversarial Networks (GANs) (Guan et al., 2023; Wang et al., 2023; Zhang
046 et al., 2023b; Zhong et al., 2023) synthesize talking avatars conditioned on audio or landmarks,
047 but often suffer from identity inconsistency and inter-frame jitter (Peng et al., 2024), undermining
048 overall realism and temporal stability. Methods based on Neural Radiance Fields (NeRFs) (Milden-
049 hall et al., 2021; Guo et al., 2021; Shen et al., 2022; Yao et al., 2022) improve structural modeling
050 through volumetric rendering, yet frequently exhibit facial collapse, loss of fine-grained details, and
051 poor lip-speech synchronization. Recently, 3D Gaussian Splatting (3DGS) (Kerbl et al., 2023) has
052 emerged as a compelling alternative due to its efficient rendering and strong spatial modeling ca-
053 pabilities. However, existing 3DGS-based methods (Cho et al., 2024; He et al., 2024; Li et al.,
054 2024) still struggle with expression jitter, temporal incoherence, and imprecise lip synchronization,
055 limiting both fidelity and controllability.

To overcome low fidelity and limited controllability in audio-driven avatars, we revisit key limitations of existing methods. NeRF- and 3DGS-based approaches rely heavily on traditional sinusoidal positional encoding, which fails to capture local spatial variations and causes facial collapse with loss of fine details. More broadly, GAN-, NeRF-, and 3DGS-based methods suffer from temporal misalignment between audio and expression features, leading to lip-sync errors and discontinuous expressions, as well as the independent treatment of expression and head pose, which produces rigid motion and poor controllability. Inspired by these limitations, we introduce Talk2Me, a 3DGS-based framework tailored to enhance visual fidelity and enable controllable facial and head dynamics. Built upon 3DGS, Talk2Me incorporates several targeted modules to address the identified challenges.

Facial collapse and the loss of fine-grained details are two key obstacles to high-fidelity avatar generation. We address these issues by reforming the avatar modeling framework with Learnable Positional Encoding (LPE) and a modified Region-Weighted Mechanism, which more effectively capture spatial relationships among Gaussian primitives and improve structural consistency and detail preservation. To further improve controllability over expressive dynamics, we incorporate the Eye Aspect Ratio (EAR) (Dewi et al., 2022) feature into the expression representation, enabling fine-grained modulation of blinking. It is also worth noting that the inherent modeling capability of 3DGS naturally ensures identity consistency throughout the animation process.

For expression controllability, we introduce an Expression Generator (EG) equipped with an Audio-Expression Temporal Fusion (AETF) module. This component jointly models audio and expression features across time, enabling accurate lip synchronization and smooth expression transitions. A region-aware attention mechanism further refines lip and eye details, enriching facial features and improving lip-sync precision.

For pose controllability, we introduce a Retrieval-Based Pose Generator (RBPG) alongside a dedicated Pose Refiner (PR), which jointly generate natural and expressive head movements. PR takes the retrieved pose, expression, and audio features as input, performing structured cross-modal fusion and temporal modeling via multi-layer transformers. By capturing the intrinsic correlation between expressions and head motion and optimizing temporal dynamics, our method ensures coherent and lifelike head behavior. Furthermore, to assess cross-lingual generalization, we curate a Mandarin video dataset featuring diverse identities and speech content.

Leveraging the above strategies, Talk2Me achieves high-fidelity, expressive, and controllable avatar synthesis, with precise lip synchronization, natural head motion, and robust facial detail preservation. Evaluations on both English and Mandarin datasets confirm its superiority over existing methods in generation quality, synchronization accuracy, motion coherence, and expression controllability.

Our main contributions are summarized as follows:

- We present Talk2Me, an audio-driven avatar framework designed to improve both visual fidelity and motion controllability in expressive talking head synthesis.
- We enhance 3D Gaussian Splatting with a Learnable Positional Encoding (LPE) and a modified Region-Weighted Mechanism, effectively addressing facial collapse and enabling fine-grained expression control.
- We propose an Expression Generator (EG) for expressive and controllable facial expression synthesis, and a Retrieval-Based Pose Generator (RBPG) to model expression–pose correlation, enhancing head motion naturalness and controllability.
- Extensive experiments on both English and Mandarin corpus show that Talk2Me delivers more faithful and controllable talking avatars than existing methods.

2 RELATED WORK

GAN-BASED METHODS.

Early works (Chen et al., 2018; Prajwal et al., 2020; Sun et al., 2022; Guan et al., 2023; Wang et al., 2023; Zhong et al., 2023) focus on synthesizing only the mouth region. Although they achieve accurate lip synchronization, they often neglect identity preservation. Later works (Chen et al., 2019; Das et al., 2020) expand to full-face generation to address visual discontinuities, but identity

108 drift and inter-frame jitter still remain. More recent efforts (Song et al., 2022; KR et al., 2019;
 109 Zhou et al., 2020; Lu et al., 2021; Ji et al., 2022; Zhang et al., 2023a; 2021a; Zhou et al., 2021)
 110 incorporate head pose, blinking, and emotion to improve expressiveness. However, due to frame-
 111 wise generation and the absence of temporal constraints, these models still struggle to ensure visual
 112 fidelity and controllable motion. In contrast, Talk2Me leverages the 3DGS representation to ensure
 113 identity consistency, high-fidelity rendering, and temporally coherent control.

114 **NERF-BASED METHODS.**

115 NeRF-based methods improve identity consistency and spatial coherence over 2D GANs, enabling
 116 higher-quality talking avatars. Yet, early audio-driven NeRFs often suffer from facial collapse and
 117 detail loss, degrading fidelity and lip synchronization. Subsequent works attempt to mitigate these
 118 issues—AD-NeRF (Guo et al., 2021) drives NeRFs directly from audio, DFA-NeRF (Yao et al.,
 119 2022) decouples facial attributes, and SSP-NeRF (Liu et al., 2022) introduces semantic-aware mod-
 120 eling. To enhance efficiency, RAD-NeRF (Tang et al., 2025) and ER-NeRF (Li et al., 2023)
 121 accelerate training and rendering, while SyncTalk (Peng et al., 2024) emphasizes precise lip–pose
 122 synchronization. Despite these advances, challenges remain in reconstructing high-frequency facial
 123 details (especially lips), avoiding subtle collapse, and achieving fine-grained controllability. In con-
 124 trast, Talk2Me builds on 3DGS with LPE and couples expression representation with EAR to ensure
 125 high fidelity and controllable expression dynamics.

126 **3DGS-BASED METHODS.**

127 Recent advances in 3D Gaussian Splatting (3DGS) have demonstrated strong capabilities in scene
 128 modeling and efficient rendering, making it increasingly popular for audio-driven avatar synthesis.
 129 Pioneering works such as EmoTalk3D (He et al., 2024), GaussianTalker Cho et al. (2024), and
 130 TalkingGaussian (Li et al., 2024) have begun to explore this direction, with a particular focus on
 131 accelerating the rendering process. However, these methods often lack explicit temporal modeling
 132 between audio signals and expression features, leading to common issues such as expression jitter,
 133 lip-sync mismatches, and overall temporal incoherence. These shortcomings ultimately limit the
 134 realism and controllability of the generated avatars.

135 Unlike previous 3DGS-based methods, Talk2Me introduces EG to generate temporally coherent and
 136 controllable facial expressions while improving lip-sync accuracy. In addition, it incorporates RBPG
 137 to explicitly model the correlation between facial expression and head pose, leading to more natural
 138 and controllable head movements.

139 **3 PRELIMINARY**

140 **3.1 3D GAUSSIAN SPLATTING.**

141 3D Gaussian Splatting (3DGS) is a real-time rendering method that models a scene with a set of
 142 anisotropic 3D Gaussian primitives. Each primitive is parameterized by a spatial center $\mu \in \mathbb{R}^3$,
 143 scale s , rotation q , feature vector z , color c , and opacity α . These primitives collectively encode the
 144 geometry, appearance, and transparency of the scene.

145 Unlike NeRF-based methods relying on dense ray marching, 3DGS treats each Gaussian as an el-
 146 liptical blob projected onto the screen and blended via differentiable rasterization, achieving high-
 147 quality, real-time rendering.

148 Given N Gaussians $\{G_i\}_{i=1}^N$, the pixel color is obtained by alpha-compositing weighted Gaussians:

$$149 \quad C = \sum_{i=1}^N w_i \cdot c_i, \quad \text{where} \quad w_i = \alpha_i \cdot T_i \quad (1)$$

150 where T_i is the transmittance term accounting for occlusion and depth.

151 3DGS supports end-to-end optimization of geometry and appearance. However, directly applying it
 152 to talking head synthesis can cause facial collapse or detail loss under large deformations, motivating
 153 our improvements.

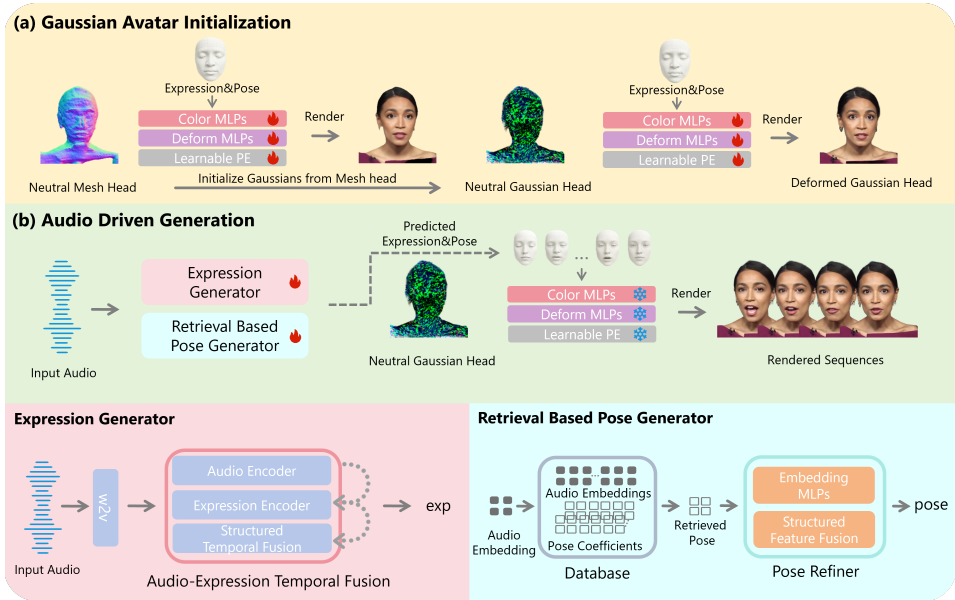


Figure 1: **Overview of Talk2Me.** Our framework has two stages: (a) Gaussian Avatar Initialization, where a mesh-based talking head initializes a 3D Gaussian avatar; (b) Audio-Driven Generation, where the Expression Generator (EG) and Retrieval-Based Pose Generator (RBPG) predict expressions and poses from audio to produce expressive, temporally coherent renderings.

4 METHOD

4.1 OVERVIEW

In this section, we present the proposed *Talk2Me*, as illustrated in Figure 1. It comprises two stages: (a) *Gaussian Avatar Initialization*, which builds a 3D Gaussian head from a mesh-based avatar, and (b) *Audio-Driven Generation*, where the Expression Generator (EG) and Retrieval-Based Pose Generator (RBPG) predict expression and pose from input audio to drive avatar animation. The internal designs of EG and RBPG are shown at the bottom of Figure 1, and we describe each module in detail below. For more detailed model designs, please refer to the Appendix A.3.

4.2 GAUSSIAN AVATAR INITIALIZATION

Following HHAvtor (Liao et al., 2023), we use DMTet to extract a neutral mesh head, which serves as the foundation for initializing 3D Gaussian primitives in a canonical space.

4.2.1 REGION-WEIGHTED MECHANISM.

We aim to build an animatable Gaussian Avatar driven by expression e and head pose p . Given audio, we predict temporally aligned e and p to deform Gaussian primitives for expressive, high-fidelity animation.

To balance local expressivity and global stability, we adapt the region-weighted mechanism from HHAvtor (Liao et al., 2023), integrating expression features. Facial regions near landmarks (e.g., mouth, eyes) are assigned higher expression weights

$$w_{\text{exp}} = \text{clamp} \left(\frac{d_{\text{far}} - d}{d_{\text{far}} - d_{\text{near}}}, 0, 1 \right), \quad (2)$$

where d is the distance to the nearest neutral landmark, and $w_{\text{pose}} = 1 - w_{\text{exp}}$. Thus, expressive regions mainly follow e (augmented with EAR for ocular details), while peripheral regions follow p for coherent global motion.

216 We implement controllable deformation using an MLP-based network ϕ_D that takes primitive fea-
 217 tures \mathbf{z} , expression \mathbf{e} , pose \mathbf{p} , and ocular-aware features β , and outputs attribute offsets:

$$218 \quad (219) \quad (\mu', \mathbf{s}', \mathbf{q}', \mathbf{c}', \alpha') = \phi_D(\mu, \mathbf{s}, \mathbf{q}, \mathbf{c}, \alpha; \mathbf{e}, \mathbf{p}, \mathbf{z}, \beta). \quad (3)$$

220 The updated primitives are rendered by a differentiable rasterizer:

$$221 \quad I = \mathcal{R}(\mu', \mathbf{s}', \mathbf{q}', \mathbf{c}', \alpha'), \quad (4)$$

223 producing temporally aligned, expressive, and controllable Gaussian Avatars.

225 4.2.2 LEARNABLE POSITIONAL ENCODING.

227 To enhance deformation accuracy in dynamic facial regions, we introduce a hybrid positional en-
 228 coding that integrates explicit coordinates, sinusoidal features, and a learnable position table. For
 229 each Gaussian primitive i with coordinate \mathbf{x}_i , we compute a linear coordinate embedding $\text{PC}(\mathbf{x}_i)$
 230 and an index-based sinusoidal encoding

$$231 \quad S(i) = [\sin(i \cdot (\gamma \odot \mathbf{f}) + \phi), \cos(i \cdot (\gamma \odot \mathbf{f}) + \phi)], \quad (5)$$

232 where \mathbf{f} is the frequency band vector, γ a learnable global scale, and ϕ a learnable phase. A learnable
 233 positional table $L(i)$ further models local offsets, and we blend them as:

$$235 \quad \tilde{P}(i) = \sigma(\alpha) L(i) + (1 - \sigma(\alpha)) S(i). \quad (6)$$

236 The final feature is:

$$237 \quad \mathbf{z}_i = \text{PC}(\mathbf{x}_i) + \tilde{P}(i). \quad (7)$$

239 This design provides complementary benefits: $\text{PC}(\mathbf{x}_i)$ encodes geometric priors, $S(i)$ captures mul-
 240 tiscale frequency information with adaptive band distribution, and $L(i)$ learns local nonlinear devi-
 241 tions. The sigmoid-controlled blending ensures a smooth trade-off between global Fourier priors
 242 and local corrections, yielding better modeling of complex deformations in regions such as eyes.

243 4.3 AUDIO-DRIVEN GAUSSIAN AVATAR

245 To enable high-fidelity and controllable talking head synthesis, we extend the neutral Gaussian
 246 Avatar by incorporating audio-driven dynamics. Our framework introduces two key modules: the
 247 *Expression Generator* (EG) and the *Retrieval-Based Pose Generator* (RBPG), which respectively
 248 predict temporally aligned facial expressions and head poses from audio. These modules collabora-
 249 tively produce synchronized, expressive, and naturalistic animations.

251 4.3.1 EXPRESSION GENERATOR.

253 Mapping speech to coherent facial animation is challenging due to the intricate coupling between
 254 phonetic content and facial dynamics. Our Expression Generator (EG) addresses this with two key
 255 modules: *Audio-Expression Temporal Fusion* (AETF) and a *Region-Aware Attention Mechanism*.

256 *Audio-Expression Temporal Fusion*. As shown in Figure 1 (bottom-left, pink), AETF comprises
 257 an Audio Encoder, an Expression Encoder, and a Structured Temporal Fusion block. The Audio
 258 Encoder extracts phonetic and emotional cues from a pretrained Wav2Lip model, while the Express-
 259 ion Encoder derives style features from a reference frame. Both are projected into a shared latent
 260 space, where the fusion block models their temporal interplay for context-aware, audio-aligned ex-
 261 pressions.

262 To capture second-order interactions, we propose a *K-product fusion* mechanism. Given audio \mathbf{a} ,
 263 emotion \mathbf{e} , and style \mathbf{s} features, their pairwise Kronecker products are projected as

$$264 \quad f_e = \phi_E(\mathbf{a} \otimes \mathbf{e}, \mathbf{a} \otimes \mathbf{s}, \mathbf{e} \otimes \mathbf{s}), \quad (8)$$

265 where ϕ_E is a learnable projection. The fused representation is refined via gated concatenation and
 266 fed into a Transformer-based temporal encoder, yielding smooth expression trajectories.

268 *Region-Aware Attention Mechanism*. To improve fidelity in perceptually critical areas, we adopt
 269 a region-aware decoding strategy. A global decoder predicts full-face expressions, while a multi-
 270 head attention module refines region-specific dynamics (e.g., eyes) over fused temporal features.

270 Their outputs are merged into a unified representation, ensuring both lips and eyes exhibit precise,
 271 synchronized motion.

272 We further employ a dual-pathway design to balance phoneme responsiveness and contextual ex-
 273 pressiveness. The main pathway leverages AETF to produce emotion- and style-aware features,
 274 while a parallel direct audio-to-expression stream captures sharp, phoneme-synchronous lip move-
 275 ments. The two are fused and passed through a lightweight temporal smoothing layer, yielding
 276 expressive, temporally stable facial animation.

277 **4.3.2 RETRIEVAL-BASED POSE GENERATOR.**

278 Most methods neglect the correlation between head motion and facial expression, causing unsta-
 279 ble dynamics despite accurate lip-sync. We address this with the *Retrieval-Based Pose Genera-
 280 tor (RBPG)*, which grounds pose in real motion data and refines it with expression–audio cues for
 281 smooth, speech-synchronized trajectories.

282 Given a monocular talking video of the target, we build an audio–pose database \mathcal{D} segmented into
 283 N -frame units. At inference, the input audio is encoded to \mathbf{a}' and matched via cosine similarity to
 284 retrieve an initial pose $\hat{\mathbf{p}}$.

285 *Pose Refiner.* To refine $\hat{\mathbf{p}}$, we fuse it with expression features \mathbf{e}' via a Kronecker-product interaction:

$$f_p = \phi_p(\hat{\mathbf{p}} \otimes \mathbf{e}'), \quad (9)$$

286 where ϕ_p is a learnable fusion network. A cross-attention block then incorporates audio \mathbf{a}' to align
 287 pose with speech prosody. A Transformer decoder subsequently predicts residual corrections $\Delta\mathbf{p}$,
 288 producing the final pose $\mathbf{p} = \hat{\mathbf{p}} + \Delta\mathbf{p}$.

289 This retrieval–refinement framework yields head motions that are temporally smooth, expression-
 290 consistent, and synchronized with speech. The detailed architecture of Pose Refiner is illustrated in
 291 Figure 12.

292 **4.4 TRAINING DETAILS**

293 *Gaussian Avatar.* To achieve high-fidelity facial rendering, we augment standard 3DGS optimization
 294 with additional perceptual and adversarial objectives. In addition to \mathcal{L}_1 , perceptual loss \mathcal{L}_p , and
 295 SSIM loss \mathcal{L}_s , we include an adversarial loss \mathcal{L}_a to improve realism. The overall objective is:

$$\mathcal{L}_A = \lambda_1 \mathcal{L}_1 + \lambda_p \mathcal{L}_p + \lambda_s \mathcal{L}_s + \lambda_a \mathcal{L}_a. \quad (10)$$

306 *Expression Generator.* EG is trained with a weighted \mathcal{L}_1 loss between predicted $\hat{\mathbf{e}}$ and ground truth
 307 \mathbf{e} , assigning higher weights \mathbf{w} to eye-related coefficients:

$$\mathcal{L}_E = \lambda_e \cdot \mathcal{L}_1(\hat{\mathbf{e}}, \mathbf{e}; \mathbf{w}). \quad (11)$$

308 *Retrieval-Based Pose Generator.* RBPG learns speech- and expression-conditioned head pose se-
 309 quences with temporal coherence. A dual-branch discriminator evaluates realism globally and lo-
 310 cally. The generator loss combines adversarial, reconstruction, and velocity smoothness terms:

$$\mathcal{L}_P = \lambda_{gan} \mathcal{L}_{gan} + \lambda_{rec} \mathcal{L}_1(\mathbf{p}, \hat{\mathbf{p}}) + \lambda_{vel} \mathcal{L}_1(\mathbf{v}, \mathbf{0}), \quad (12)$$

311 where $\mathbf{v}_t = \hat{\mathbf{p}}_t - \hat{\mathbf{p}}_{t-1}$ enforces smooth motion, and $\lambda_{rec} = 10.0$, $\lambda_{vel} = 1.0$.

314 **5 EXPERIMENTS**

316 **5.1 EXPERIMENT SETTINGS**

318 **5.1.1 DATASET.**

320 We utilize monocular talking videos from the HDTF (Zhang et al., 2021b) dataset for training
 321 and evaluation. To test cross-lingual generalization, we additionally collect 25 Mandarin videos
 322 from diverse identities. Backgrounds are removed using the method in (Lin et al., 2022) to isolate
 323 portrait regions. Following prior work, all videos are center-cropped and resized to 512×512 , with
 a fixed frame rate of 25 FPS.

324 5.1.2 COMPARISON BASELINES.
325326 We compare with GAN-based methods (Wav2Lip (Prajwal et al., 2020), VideoReTalking (Cheng
327 et al., 2022), IP-LAP (Zhong et al., 2023)), NeRF-based methods (ER-NeRF (Li et al., 2023),
328 SyncTalk (Peng et al., 2024), Real3D-Portrait (Ye et al., 2024b), MimicTalk (Ye et al., 2024a)),
329 and 3DGS-based methods (GaussianTalker (Cho et al., 2024), TalkingGaussian (Li et al., 2024)).
330331 5.1.3 IMPLEMENTATION DETAILS.
332333 Our method follows a three-stage training pipeline. We first train a neutral mesh head for 30,000
334 steps, then use it to initialize the Gaussian Avatar, which is further optimized for 20,000 steps. The
335 Expression Generator (EG) and the generator of the Retrieval-Based Pose Generator (RBPG) are
336 trained jointly for 2,000 epochs with a learning rate of 1×10^{-4} , while the RBPG discriminator uses
337 a learning rate of 1×10^{-3} . Training completes within a few hours on a single RTX A6000 GPU.
338339 5.2 QUANTITATIVE EVALUATION
340341 5.2.1 RECONSTRUCTION QUALITY ASSESSMENT.
342343 Following (Li et al., 2023; Cho et al., 2024), we evaluate identity-specific reconstruction on the test
344 set using the audio from the original video. Metrics include PSNR, LPIPS (Zhang et al., 2018), FID
345 (Heusel et al., 2017), MS-SSIM, and Landmark Distance (LMD), measuring photometric accuracy,
346 perceptual realism, and geometric alignment.
347348 5.2.2 AUDIO DRIVEN QUALITY ASSESSMENT.
349350 For audio-driven evaluation, where facial and head motions vary, pixel-level metrics are less reliable.
351 We follow Wav2Lip (Prajwal et al., 2020) and report Lip Sync Error Distance (LSE-D) and Lip Sync
352 Confidence (LSE-C) to assess lip–speech alignment using audio from a different video.
353354 5.2.3 EVALUATION RESULTS.
355356 **Table 1: Quantitative evaluation of reconstruction and audio-driven talking head synthesis.**
357 We evaluate the methods using standard metrics for visual quality (PSNR, LPIPS, MS-SSIM, FID,
358 LMD) and audio-visual synchronization (LSE-D, LSE-C). **Bold** and underlined indicate the best
and second-best results, respectively.

Methods	Reconstruction							Audio Driven	
	PSNR↑	LPIPS↓	MS-SSIM↑	FID↓	LMD↓	LSE-D↓	LSE-C↑	LSE-D↓	LSE-C↑
GAN	Wav2Lip	32.565	0.027	0.986	5.685	2.755	6.673	8.922	8.819
	VideoReTalking	32.828	0.031	0.983	<u>5.329</u>	2.978	6.556	8.634	8.889
	IP-LAP	<u>33.107</u>	0.024	0.991	5.791	2.789	<u>6.420</u>	8.941	9.498
NeRF	ER-NeRF	30.939	0.027	0.983	9.514	2.598	6.935	8.597	10.191
	SyncTalk	36.449	<u>0.023</u>	0.962	6.243	2.265	8.434	6.910	9.140
	Real3DPortrait	21.709	0.090	0.895	28.871	5.038	6.945	8.364	10.442
	MimicTalk	23.233	0.064	0.979	19.638	5.239	8.353	6.827	4.619
3DGS	GaussianTalker	28.217	0.048	0.981	21.549	<u>2.306</u>	7.797	7.863	11.841
	TalkingGaussian	30.944	0.027	<u>0.987</u>	9.266	2.592	6.939	8.568	9.572
	Talk2Me	29.489	0.018	0.976	5.082	3.437	6.300	8.993	8.757

370 Quantitative results for avatar reconstruction and audio-driven synthesis are shown in Table 1, comparing
371 **Talk2Me** with recent GAN-, NeRF-, and 3DGS-based methods. Under the reconstruction
372 setting, **Talk2Me** achieves state-of-the-art perceptual quality (LPIPS, FID) and the best lip–speech
373 synchronization (LSE-D/C). Within the 3DGS family, it clearly outperforms *GaussianTalker* on per-
374 ceptual metrics, indicating more realistic rendering and tighter audio–visual alignment, while pre-
375 serving 3D consistency. Although our method does not lead in PSNR or MS-SSIM, this is expected
376 given our *full-head generation* strategy. Unlike models that only edit the mouth in static frames,
377 we synthesize full-face dynamics and head motion—variations that enhance realism and synchro-
378 nization but may be penalized by pixel-level metrics. In the audio-driven setting, **Talk2Me** achieves

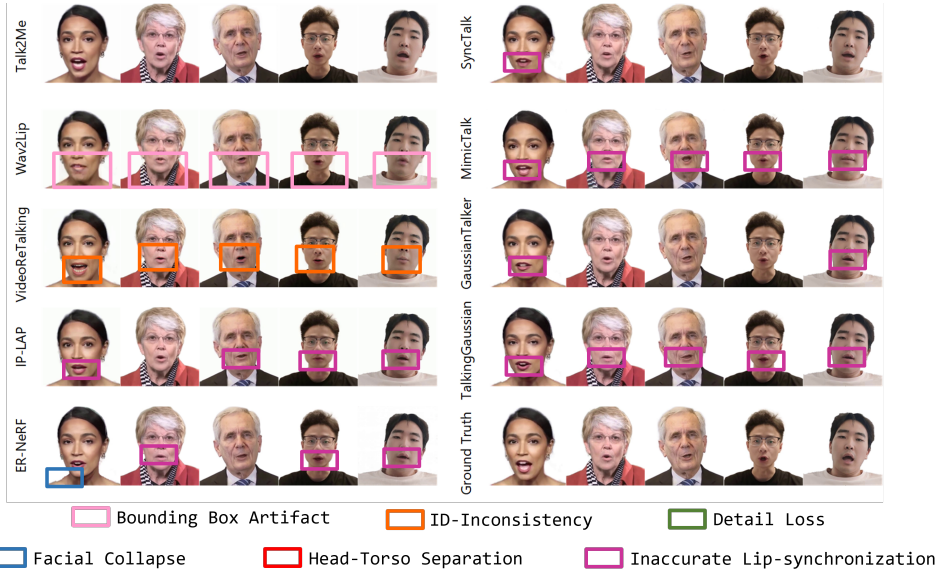


Figure 2: **Qualitative comparison of facial synthesis by different methods.** Compared with GAN-, NeRF-, and 3DGS-based baselines, Talk2Me achieves more accurate lip synchronization, richer facial expressions, and better identity preservation. The results closely match the ground truth (bottom-right) while avoiding artifacts like facial collapse. Please zoom in for details.

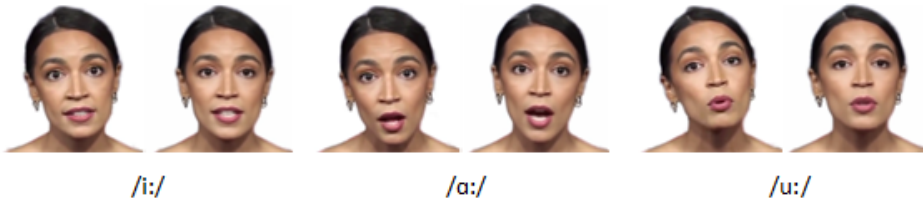


Figure 3: **Head pose diversity with the same audio.** Talk2Me produces natural, diverse head movements while preserving accurate lip-sync. Left: Ground Truth; Right: ours.

the best synchronization across all metrics. Overall, our method delivers high-fidelity, speech-aware animation with fine-grained perceptual detail, controllable expressions, and natural motion.

5.3 QUALITATIVE EVALUATION

5.3.1 VISUALIZATION RESULTS.

Figure 2 shows a qualitative comparison across GAN-, NeRF-, and 3DGS-based methods. **Talk2Me** generates expressive facial details, including accurate lip movements and natural head motion, while preserving identity and structural coherence. Unlike GAN-based methods that often distort identity, or NeRF-based ones prone to facial collapse, our method generates fine-grained expression and pose that are well aligned with speech, enabling high-fidelity, controllable, audio driven facial animation. A more detailed comparison is provided in the Appendix A.2.1 and supplementary material.

5.3.2 HEAD POSE GENERATION.

Figure 3 demonstrates **Talk2Me**’s ability to generate natural, diverse head motion from audio while maintaining accurate lip synchronization. Unlike methods that require external driving videos, it predicts temporally coherent head dynamics and expressions directly from speech, enabling fully audio-driven motion.

432
 433 **Table 2: User study (ratings 1–5) on five aspects.** **Bold** and underlined indicate the best and
 434 second-best results, respectively.

	Methods	Lip-sync	Expression-sync	Pose-sync	Image quality	Video realness
436 437 438 439 440 441 442 443 444	436 437 438 439 440 441 442 443 444 445 446 447 448 449 450 451 452 453 454 455 456 457 458 459 460 461 462 463 464 465 466 467 468 469 470 471 472 473 474 475 476 477 478 479 480 481 482 483 484 485	436 437 438 439 440 441 442 443 444 445 446 447 448 449 450 451 452 453 454 455 456 457 458 459 460 461 462 463 464 465 466 467 468 469 470 471 472 473 474 475 476 477 478 479 480 481 482 483 484 485 Wav2Lip VideoReTalking IP-LAP ER-NeRF SyncTalk Real3DPORtrait MimicTalk GaussianTalker TalkingGaussian Talk2Me	436 437 438 439 440 441 442 443 444 445 446 447 448 449 450 451 452 453 454 455 456 457 458 459 460 461 462 463 464 465 466 467 468 469 470 471 472 473 474 475 476 477 478 479 480 481 482 483 484 485 3.89 3.72 <u>4.17</u> 3.18 3.83 3.15 3.60 3.56 3.82 4.54 4.04 3.85 <u>4.07</u> 3.26 3.93 3.11 3.23 3.63 3.87 4.50 4.11 3.97 3.97 3.23 3.89 3.08 3.50 3.64 4.00 4.49 3.71 3.72 4.00 3.08 3.89 2.84 3.56 3.41 3.74 3.81 3.98 3.66 4.00 3.18 3.65 3.04 3.57 3.42 3.85 4.47	436 437 438 439 440 441 442 443 444 445 446 447 448 449 450 451 452 453 454 455 456 457 458 459 460 461 462 463 464 465 466 467 468 469 470 471 472 473 474 475 476 477 478 479 480 481 482 483 484 485 3.71 3.72 4.00 3.08 3.89 2.84 3.56 3.41 3.74 3.81 3.98 3.66 4.00 3.18 3.65 3.04 3.57 3.42 3.85 4.47	436 437 438 439 440 441 442 443 444 445 446 447 448 449 450 451 452 453 454 455 456 457 458 459 460 461 462 463 464 465 466 467 468 469 470 471 472 473 474 475 476 477 478 479 480 481 482 483 484 485 9	436 437 438 439 440 441 442 443 444 445 446 447 448 449 450 451 452 453 454 455 456 457 458 459 460 461 462 463 464 465 466 467 468 469 470 471 472 473 474 475 476 477 478 479 480 481 482 483 484 485 3.98 3.66 4.00 3.18 3.65 3.04 3.57 3.42 3.85 4.47

445
 446
 447 **Table 3: Ablation study of key components.** We report reconstruction and synchronization metrics.
 448 “–” denotes reconstruction metrics not applicable when RBPG generates poses autonomously.

Methods	LSE-D↓	LSE-C↑	PSNR↑	LPIPS↓	MS-SSIM↑	FID↓	LMD↓
w/o LPE, EG, RBPG	9.853	4.948	<u>25.912</u>	0.036	0.946	<u>16.018</u>	5.280
w/o LPE	8.067	7.011	-	-	-	-	-
w/o EG	9.897	5.009	-	-	-	-	-
w/o RBPG	7.994	<u>7.102</u>	26.645	0.027	0.959	13.712	3.716
Talk2Me	7.949	7.162	-	-	-	-	-

5.3.3 USER STUDY.

To assess perceptual quality, we conduct a user study following the Mean Opinion Score (MOS) protocol across five criteria. As shown in Table 2, **Talk2Me** tops four of five aspects, especially audiovisual coherence and expressiveness, and delivers overall balanced, high-fidelity, audio-synchronized facial animation despite slightly lower raw image quality. For more details, please refer to Appendix A.4.

5.4 ABLATION STUDY.

To assess the contribution of each component, we conduct an ablation study (Table 3). Removing any module degrades performance, confirming its necessity. Removing LPE affects geometric deformation, which in turn reduces lip-sync accuracy, highlighting its role in audio-visual alignment. Excluding EG causes larger drops, underscoring the importance of the fusion design for temporal consistency. The comparison between rows 1 and 4 further indicates that LPE and EG enhance image quality, demonstrating the effectiveness of learnable spatial encoding and audio-expression alignment. We further compare LPE with the conventional sinusoidal encoding from multiple perspectives, please refer to Appendix A.2.2 for details. In addition, we further investigate the impact of each loss term on model performance, with more details provided in Appendix A.2.3.

6 CONCLUSION

In this paper, we present Talk2Me, a high-fidelity and controllable audio-driven avatar framework that advances realistic talking head synthesis. Built upon 3D Gaussian Splatting, Talk2Me introduces a learnable spatial encoding and a modified region-weighted mechanism to preserve facial detail and structure. Our Expression Generator and Retrieval-Based Pose Generator jointly model audio-expression-pose correlations, enabling synchronized lip motion, expressive facial dynamics, and natural head movement. Extensive evaluations demonstrate that Talk2Me achieves superior performance across photorealism, synchronization accuracy, and motion expressiveness, offering a robust solution for audio-driven avatar generation.

486 REFERENCES
487

488 Lele Chen, Zhiheng Li, Ross K Maddox, Zhiyao Duan, and Chenliang Xu. Lip movements gen-
489 eration at a glance. In *Proceedings of the European conference on computer vision (ECCV)*, pp.
490 520–535, 2018.

491 Lele Chen, Ross K Maddox, Zhiyao Duan, and Chenliang Xu. Hierarchical cross-modal talking
492 face generation with dynamic pixel-wise loss. In *Proceedings of the IEEE/CVF conference on*
493 *computer vision and pattern recognition*, pp. 7832–7841, 2019.

494 Kun Cheng, Xiaodong Cun, Yong Zhang, Menghan Xia, Fei Yin, Mingrui Zhu, Xuan Wang, Jue
495 Wang, and Nannan Wang. Videoretalking: Audio-based lip synchronization for talking head
496 video editing in the wild. In *SIGGRAPH Asia 2022 Conference Papers*, pp. 1–9, 2022.

497 Kyusun Cho, Joungbin Lee, Heeji Yoon, Yeobin Hong, Jaehoon Ko, Sangjun Ahn, and Seungry-
498 ong Kim. Gaussiantalker: Real-time high-fidelity talking head synthesis with audio-driven 3d
499 gaussian splatting. *arXiv preprint arXiv:2404.16012*, 2024.

500 Joon Son Chung and Andrew Zisserman. Out of time: automated lip sync in the wild. In *Asian*
501 *conference on computer vision*, pp. 251–263. Springer, 2016.

502 Dipanjan Das, Sandika Biswas, Sanjana Sinha, and Brojeshwar Bhowmick. Speech-driven facial
503 animation using cascaded gans for learning of motion and texture. In *European conference on*
504 *computer vision*, pp. 408–424. Springer, 2020.

505 Christine Dewi, Rung-Ching Chen, Xiaoyi Jiang, and Hui Yu. Adjusting eye aspect ratio for strong
506 eye blink detection based on facial landmarks. *PeerJ Computer Science*, 8:e943, 2022.

507 Jiazh Guan, Zhanwang Zhang, Hang Zhou, Tianshu Hu, Kaisiyuan Wang, Dongliang He, Haocheng
508 Feng, Jingtuo Liu, Errui Ding, Ziwei Liu, et al. Stylesync: High-fidelity generalized and personal-
509 ized lip sync in style-based generator. In *Proceedings of the IEEE/CVF Conference on Computer*
510 *Vision and Pattern Recognition*, pp. 1505–1515, 2023.

511 Yudong Guo, Keyu Chen, Sen Liang, Yong-Jin Liu, Hujun Bao, and Juyong Zhang. Ad-nerf: Au-
512 dio driven neural radiance fields for talking head synthesis. In *Proceedings of the IEEE/CVF*
513 *international conference on computer vision*, pp. 5784–5794, 2021.

514 Qianyun He, Xinya Ji, Yicheng Gong, Yuanxun Lu, Zhengyu Diao, Linjia Huang, Yao Yao, Siyu
515 Zhu, Zhan Ma, Songcen Xu, et al. Emotalk3d: high-fidelity free-view synthesis of emotional 3d
516 talking head. In *European Conference on Computer Vision*, pp. 55–72. Springer, 2024.

517 Martin Heusel, Hubert Ramsauer, Thomas Unterthiner, Bernhard Nessler, and Sepp Hochreiter.
518 Gans trained by a two time-scale update rule converge to a local nash equilibrium. *Advances in*
519 *neural information processing systems*, 30, 2017.

520 Xinya Ji, Hang Zhou, Kaisiyuan Wang, Qianyi Wu, Wayne Wu, Feng Xu, and Xun Cao. Eamm:
521 One-shot emotional talking face via audio-based emotion-aware motion model. In *ACM SIG-*
522 *GRAPH 2022 conference proceedings*, pp. 1–10, 2022.

523 Tero Karras, Samuli Laine, and Timo Aila. A style-based generator architecture for generative
524 adversarial networks. In *Proceedings of the IEEE/CVF conference on computer vision and pattern*
525 *recognition*, pp. 4401–4410, 2019.

526 Bernhard Kerbl, Georgios Kopanas, Thomas Leimkühler, and George Drettakis. 3d gaussian splat-
527 ting for real-time radiance field rendering. *ACM Trans. Graph.*, 42(4):139–1, 2023.

528 Prajwal KR, Rudrabha Mukhopadhyay, Jerin Philip, Abhishek Jha, Vinay Namboodiri, and
529 CV Jawahar. Towards automatic face-to-face translation. In *Proceedings of the 27th ACM in-*
530 *ternational conference on multimedia*, pp. 1428–1436, 2019.

531 Jiahe Li, Jiawei Zhang, Xiao Bai, Jun Zhou, and Lin Gu. Efficient region-aware neural radiance
532 fields for high-fidelity talking portrait synthesis. In *Proceedings of the IEEE/CVF International*
533 *Conference on Computer Vision*, pp. 7568–7578, 2023.

540 Jiahe Li, Jiawei Zhang, Xiao Bai, Jin Zheng, Xin Ning, Jun Zhou, and Lin Gu. Talkinggaussian:
 541 Structure-persistent 3d talking head synthesis via gaussian splatting. In *European Conference on*
 542 *Computer Vision*, pp. 127–145. Springer, 2024.

543 Zhanfeng Liao, Yuelang Xu, Zhe Li, Qijing Li, Boyao Zhou, Ruiyuan Bai, Di Xu, Hongwen Zhang,
 544 and Yebin Liu. Hhavatar: Gaussian head avatar with dynamic hairs. *arXiv e-prints*, pp. arXiv–
 545 2312, 2023.

546 Shanchuan Lin, Linjie Yang, Imran Saleemi, and Soumyadip Sengupta. Robust high-resolution
 547 video matting with temporal guidance. In *Proceedings of the IEEE/CVF Winter Conference on*
 548 *Applications of Computer Vision*, pp. 238–247, 2022.

549 Xian Liu, Yinghao Xu, Qianyi Wu, Hang Zhou, Wayne Wu, and Bolei Zhou. Semantic-aware im-
 550 plicit neural audio-driven video portrait generation. In *European conference on computer vision*,
 551 pp. 106–125. Springer, 2022.

552 Yuanxun Lu, Jinxiang Chai, and Xun Cao. Live speech portraits: real-time photorealistic talking-
 553 head animation. *ACM Transactions on Graphics (ToG)*, 40(6):1–17, 2021.

554 Ben Mildenhall, Pratul P Srinivasan, Matthew Tancik, Jonathan T Barron, Ravi Ramamoorthi, and
 555 Ren Ng. Nerf: Representing scenes as neural radiance fields for view synthesis. *Communications*
 556 *of the ACM*, 65(1):99–106, 2021.

557 Ziqiao Peng, Yihao Luo, Yue Shi, Hao Xu, Xiangyu Zhu, Hongyan Liu, Jun He, and Zhaoxin Fan.
 558 Selftalk: A self-supervised commutative training diagram to comprehend 3d talking faces. In
 559 *Proceedings of the 31st ACM International Conference on Multimedia*, pp. 5292–5301, 2023.

560 Ziqiao Peng, Wentao Hu, Yue Shi, Xiangyu Zhu, Xiaomei Zhang, Hao Zhao, Jun He, Hongyan
 561 Liu, and Zhaoxin Fan. Sync talk: The devil is in the synchronization for talking head synthesis.
 562 In *Proceedings of the IEEE/CVF Conference on Computer Vision and Pattern Recognition*, pp.
 563 666–676, 2024.

564 KR Prajwal, Rudrabha Mukhopadhyay, Vinay P Namboodiri, and CV Jawahar. A lip sync expert is
 565 all you need for speech to lip generation in the wild. In *Proceedings of the 28th ACM international*
 566 *conference on multimedia*, pp. 484–492, 2020.

567 Shuai Shen, Wanhua Li, Zheng Zhu, Yueqi Duan, Jie Zhou, and Jiwen Lu. Learning dynamic facial
 568 radiance fields for few-shot talking head synthesis. In *European conference on computer vision*,
 569 pp. 666–682. Springer, 2022.

570 Linsen Song, Wayne Wu, Chen Qian, Ran He, and Chen Change Loy. Everybody’s talkin’: Let me
 571 talk as you want. *IEEE Transactions on Information Forensics and Security*, 17:585–598, 2022.

572 Yasheng Sun, Hang Zhou, Kaisiyuan Wang, Qianyi Wu, Zhibin Hong, Jingtuo Liu, Errui Ding, Jing-
 573 dong Wang, Ziwei Liu, and Koike Hideki. Masked lip-sync prediction by audio-visual contextual
 574 exploitation in transformers. In *SIGGRAPH Asia 2022 conference papers*, pp. 1–9, 2022.

575 Jiaxiang Tang, Kaisiyuan Wang, Hang Zhou, Xiaokang Chen, Dongliang He, Tianshu Hu, Jing-
 576 tuo Liu, Ziwei Liu, Gang Zeng, and Jingdong Wang. Real-time neural radiance talking portrait
 577 synthesis via audio-spatial decomposition. *International Journal of Computer Vision*, pp. 1–12,
 578 2025.

579 Jiadong Wang, Xinyuan Qian, Malu Zhang, Robby T Tan, and Haizhou Li. Seeing what you said:
 580 Talking face generation guided by a lip reading expert. In *Proceedings of the IEEE/CVF Confer-
 581 ence on Computer Vision and Pattern Recognition*, pp. 14653–14662, 2023.

582 Shunyu Yao, RuiZhe Zhong, Yichao Yan, Guangtao Zhai, and Xiaokang Yang. Dfa-nerf: Person-
 583 alized talking head generation via disentangled face attributes neural rendering. *arXiv preprint*
 584 *arXiv:2201.00791*, 2022.

585 Zhenhui Ye, Ziyue Jiang, Yi Ren, Jinglin Liu, Jinzheng He, and Zhou Zhao. Geneface: Generalized
 586 and high-fidelity audio-driven 3d talking face synthesis. *arXiv preprint arXiv:2301.13430*, 2023.

594 Zhenhui Ye, Tianyun Zhong, Yi Ren, Ziyue Jiang, Jiawei Huang, Rongjie Huang, Jinglin Liu,
 595 Jinzheng He, Chen Zhang, Zehan Wang, et al. Mimictalk: Mimicking a personalized and ex-
 596 pressive 3d talking face in minutes. *Advances in neural information processing systems*, 37:
 597 1829–1853, 2024a.

598 Zhenhui Ye, Tianyun Zhong, Yi Ren, Jiaqi Yang, Weichuang Li, Jiawei Huang, Ziyue Jiang,
 599 Jinzheng He, Rongjie Huang, Jinglin Liu, et al. Real3d-portrait: One-shot realistic 3d talking
 600 portrait synthesis. *arXiv preprint arXiv:2401.08503*, 2024b.

602 Chenxu Zhang, Yifan Zhao, Yifei Huang, Ming Zeng, Saifeng Ni, Madhukar Budagavi, and Xiaohu
 603 Guo. Facial: Synthesizing dynamic talking face with implicit attribute learning. In *Proceedings*
 604 *of the IEEE/CVF international conference on computer vision*, pp. 3867–3876, 2021a.

605 Richard Zhang, Phillip Isola, Alexei A Efros, Eli Shechtman, and Oliver Wang. The unreasonable
 606 effectiveness of deep features as a perceptual metric. In *Proceedings of the IEEE conference on*
 607 *computer vision and pattern recognition*, pp. 586–595, 2018.

609 Wenxuan Zhang, Xiaodong Cun, Xuan Wang, Yong Zhang, Xi Shen, Yu Guo, Ying Shan, and Fei
 610 Wang. Sadtalker: Learning realistic 3d motion coefficients for stylized audio-driven single image
 611 talking face animation. In *Proceedings of the IEEE/CVF conference on computer vision and*
 612 *pattern recognition*, pp. 8652–8661, 2023a.

613 Zhimeng Zhang, Lincheng Li, Yu Ding, and Changjie Fan. Flow-guided one-shot talking face gen-
 614 eration with a high-resolution audio-visual dataset. In *Proceedings of the IEEE/CVF conference*
 615 *on computer vision and pattern recognition*, pp. 3661–3670, 2021b.

616 Zhimeng Zhang, Zhipeng Hu, Wenjin Deng, Changjie Fan, Tangjie Lv, and Yu Ding. Dinet: De-
 617 formation inpainting network for realistic face visually dubbing on high resolution video. In
 618 *Proceedings of the AAAI conference on artificial intelligence*, volume 37, pp. 3543–3551, 2023b.

619 Weizhi Zhong, Chaowei Fang, Yinqi Cai, Pengxu Wei, Gangming Zhao, Liang Lin, and Guanbin Li.
 620 Identity-preserving talking face generation with landmark and appearance priors. In *Proceedings*
 621 *of the IEEE/CVF Conference on Computer Vision and Pattern Recognition*, pp. 9729–9738, 2023.

623 Hang Zhou, Yasheng Sun, Wayne Wu, Chen Change Loy, Xiaogang Wang, and Ziwei Liu. Pose-
 624 controllable talking face generation by implicitly modularized audio-visual representation. In
 625 *Proceedings of the IEEE/CVF conference on computer vision and pattern recognition*, pp. 4176–
 626 4186, 2021.

627 Yang Zhou, Xintong Han, Eli Shechtman, Jose Echevarria, Evangelos Kalogerakis, and Dingzeyu
 628 Li. Makeltalk: speaker-aware talking-head animation. *ACM Transactions On Graphics (TOG)*,
 629 39(6):1–15, 2020.

631 A APPENDIX

634 A.1 DATASET AND BASELINE DESCRIPTIONS

636 A.1.1 DATASET DETAILS

637 Our main experiments are conducted on a selected subset of the HDTF dataset (Zhang et al., 2021b),
 638 a high-resolution talking-face corpus commonly used in prior work. The full dataset consists of 362
 639 video clips (about 15.8 hours in total), from which we choose representative samples based on
 640 speaking clarity, pose stability, and identity diversity. All selected videos are center-cropped and
 641 resized to 512×512 resolution, with a fixed frame rate of 25 FPS. Background regions are extracted
 642 using the matting technique proposed in (Lin et al., 2022). To evaluate cross-lingual generalization,
 643 we further collect 25 Mandarin-speaking video clips featuring a wide range of speakers. These
 644 videos undergo the same preprocessing steps as the HDTF subset.

645 To supplement our visual comparisons, we also include a few publicly available video samples from
 646 prior works such as GeneFace (Ye et al., 2023), AD-NeRF (Guo et al., 2021), and ER-NeRF (Li
 647 et al., 2023). These samples are used for qualitative demonstration only and are not involved in
 model any quantitative evaluation.

648 A.1.2 BASELINE METHODS
649650 To ensure a comprehensive and fair evaluation, we compare our method against a wide range of state-
651 of-the-art talking-face synthesis models spanning different representation paradigms. Specifically,
652 our baselines include GAN-based methods such as Wav2Lip (Prajwal et al., 2020), VideoReTalking
653 (Cheng et al., 2022), and IP-LAP (Zhong et al., 2023), which focus on generating realistic lip-synced
654 facial motions. We also include NeRF-based approaches like ER-NeRF (Li et al., 2023), SyncTalk
655 (Peng et al., 2024), Real3dPortrait (Ye et al., 2024b), and Mimic Talk (Ye et al., 2024a), which
656 leverage volumetric scene representations to improve 3D consistency and novel view rendering. Fi-
657 nally, we consider recent 3D Gaussian-based methods, including GaussianTalker (Cho et al., 2024)
658 and TalkingGaussian (Li et al., 2024), which explicitly model facial geometry with point-based
659 representations for efficient and photorealistic synthesis. These baselines cover both traditional and
660 emerging paradigms, enabling a thorough comparison across fidelity and controllability.661 **Wav2Lip.**
662663 This method focuses on generating talking-face videos with accurate lip synchronization for arbi-
664 trary identities under unconstrained conditions. It employs a fixed, pre-trained lip-sync discriminator
665 (based on SyncNet (Chung & Zisserman, 2016)) as a strong supervisory signal to guide the gener-
666 ator, avoiding adversarial training. This work also introduces new evaluation benchmarks and two
667 metrics—Lip Sync Error-Distance (LSE-D) and Lip Sync Error-Confidence (LSE-C)—to quanti-
668 tatively measure performance. Human evaluation results show that the generated videos achieve
669 synchronization quality comparable to real footage and are consistently preferred over those pro-
670 duced by previous methods.671 **VideoReTalking.**
672673 This method proposes a three-stage framework for audio-driven talking-head video editing in natural
674 scenes: (1) generating a face video with a canonical expression; (2) producing temporally aligned
675 lip movements from audio; and (3) enhancing realism via face restoration. Expression normalization
676 uses a fixed template as pose reference to support accurate lip motion. Final outputs are refined by
677 an identity-aware restoration network guided by a StyleGAN (Karras et al., 2019) prior. Without
678 requiring identity-specific training, the system generalizes well to unseen speakers and performs
679 robustly in the wild.680 **IP-LAP.**
681682 IP-LAP is a two-stage framework for audio-driven talking-face synthesis. It first employs a
683 Transformer-based module to predict lip and jaw landmarks from speech, incorporating reference
684 landmarks and prior poses for identity consistency. In the second stage, a rendering network gener-
685 ates face frames by warping multiple static reference images based on predicted motion, then fusing
686 them with a masked frame and sketch.687 **ER-NeRF.**
688689 To enable high-fidelity audio-driven portrait synthesis, this method proposes a region-aware con-
690 ditional neural radiance field that explicitly models the spatial contributions of different facial re-
691 gions. A tri-plane hash representation decomposes the 3D space into three orthogonal 2D planes,
692 improving rendering efficiency and reducing hash collisions by pruning empty regions. To capture
693 fine-grained correlations between facial areas and speech signals, a region attention module applies
694 cross-modal attention to produce region-aware conditioning features. In addition, a lightweight and
695 efficient adaptive pose encoding maps complex head movements into spatial coordinates.696 **SyncTalk.**
697698 This NeRF-based framework is designed for audio-driven talking-head synthesis with an emphasis
699 on spatiotemporal synchronization. It jointly addresses identity preservation, lip synchronization,
700 facial expression control, and head pose alignment through a modular architecture comprising a
701 facial synchronization controller, a head stabilization unit, and a portrait rendering module. The
controller maps audio signals to dynamic facial features via an audio-visual encoder and animation
mapper, enabling accurate lip-sync and expressive control. The stabilization unit smooths and aligns

702 head motion using tracked facial keypoints, while the rendering module corrects common NeRF
 703 artifacts to improve visual fidelity.
 704

705 **Real3dPortrait.**

706 This one-shot 3D talking-head synthesis framework generates photorealistic and animatable portraits
 707 from a single input image. It addresses challenges in identity preservation, expression fidelity, and
 708 head-torso coordination by integrating several key components. A pre-trained image-to-plane (I2P)
 709 model encodes strong 3D priors to reconstruct facial geometry, while a motion adapter modulates
 710 animation behavior based on input conditions. To enable natural torso motion and background
 711 flexibility, the system incorporates a head-torso-background super-resolution (HTB-SR) module.
 712 In audio-driven scenarios, it uses a general audio-to-motion (A2M) model to generate synchronized
 713 facial animation for previously unseen identities. Together, these components enable high-quality,
 714 identity-consistent 3D portrait synthesis in a one-shot setting.

715 **MimicTalk.**

716 MimicTalk enables personalized and expressive 3D talking-face generation by rapidly adapting
 717 to target identities and producing individualized facial motion from audio. Instead of relying on
 718 identity-specific training from scratch, it builds upon a generalized NeRF-based model and in-
 719 troduces a hybrid adaptation pipeline that disentangles and learns both static appearance and dy-
 720 namic motion characteristics from a few input samples. This approach significantly reduces training
 721 time—reportedly achieving adaptation in just minutes, over 47x faster than conventional methods.
 722 Additionally, the framework integrates an intrinsically stylized audio-to-motion module (ICS-A2M),
 723 which mimics the conversational style of a reference video while preserving the content integrity of
 724 the driving audio.

725 **GaussianTalker.**

726 Leveraging the high rendering efficiency of 3D Gaussian Splatting (3DGS), GaussianTalker en-
 727 ables real-time, audio-driven talking-head synthesis with controllable head pose. It constructs a
 728 single 3DGS representation of the head and introduces a mechanism to deform the Gaussians syn-
 729 chronously with the input speech. To enable controllability, Gaussian attributes are embedded into
 730 a shared implicit feature space, which interacts with audio features to produce temporally aligned
 731 deformation signals. A spatial audio-attention module further refines these embeddings to predict
 732 per-Gaussian offset trajectories. By enforcing local coherence and leveraging spatial priors, the
 733 system achieves stable manipulation of large sets of Gaussians with complex attributes.

734 **TalkingGaussian.**

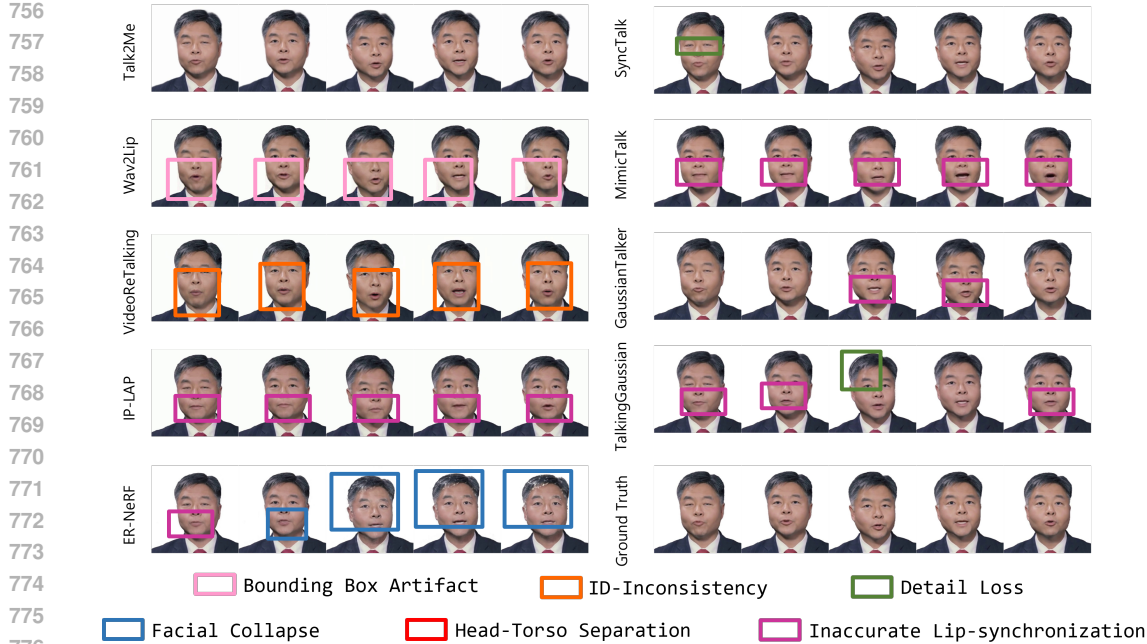
735 To address the blurriness often observed in dynamic facial regions of NeRF-based models, Talking-
 736 Gaussian introduces a structure-persistent deformation field grounded in 3D Gaussian Splatting.
 737 Smooth and continuous deformations are applied to stable Gaussian primitives, avoiding abrupt
 738 appearance transitions and resulting in clearer, more accurate head synthesis. To further enhance
 739 realism and synchronization, a motion decoupling module is incorporated to disentangle facial and
 740 oral dynamics, which simplifies training and improves lip-sync fidelity.

741 **A.2 ADDITIONAL EXPERIMENT**

742 **A.2.1 GENERALIZATION ABILITY**

743 To further evaluate the generalization and robustness of our method, we conduct additional experi-
 744 ments on a set of supplementary data samples. We compare the proposed method against all baseline
 745 methods, and report the qualitative visual performance of each method.

746 In Figures 4 and 5, we present the lip-sync performance across consecutive frames on the supple-
 747 mentary dataset. In terms of *lip-sync accuracy*, our method exhibits almost identical results to the
 748 ground truth, demonstrating the strong capability of **Talk2Me** in audio-driven talking head syn-
 749 thesis. Compared to the traditional GAN-based method **Wav2Lip**, our approach delivers superior
 750 image quality. As shown in Figures 4 and 5, Wav2Lip often produces noticeable bounding box
 751 artifacts around the mouth region. Moreover, it is visually evident that **VideoReTalking** performs



756
757
758
759
760
761
762
763
764
765
766
767
768
769
770
771
772
773
774
775
776
777
778
779
780
781
782
783
784
785
786
787
788
789
790
791
792
793
794
795
796
797
798
799
800
801
802
803
804
805
806
807
808
809

Figure 4: **Qualitative comparison of lip-sync performance on the supplementary dataset (Speaker A).** **Talk2Me** achieves superior lip-sync accuracy and identity preservation, with results close to the ground truth and fewer artifacts compared to prior GAN-, NeRF-, and 3DGS-based methods. Please zoom in for more details.

poorly in preserving speaker identity — the mouth appears to belong to a different person rather than the target identity. In contrast, **Talk2Me** maintains identity consistency remarkably well.

Compared to NeRF-based methods, our approach demonstrates significantly better preservation of fine-grained details and a more coherent connection between the head and torso. We attribute the head-torso discontinuity observed in NeRF-based methods to the *separate treatment* of these regions during the training phase.

Furthermore, in comparison to the other two 3DGS-based methods, the proposed method demonstrates more stable detail preservation and lip-sync performance across temporally continuous frames. For more intuitive and detailed comparisons, please refer to the supplementary videos provided, where we manually annotate the artifact-prone regions to better illustrate the differences.

A.2.2 DETAILED VISUALIZATION RESULTS OF LPE ABLATION

In this section, to more intuitively and thoroughly validate the effectiveness of LPE, we provide additional visualization-based ablation results from three perspectives: the geometric quality of Mesh Head, the preservation of pupil illumination in Gaussian Head, and the preservation of eye details in Gaussian Head. These experiments highlight how LPE impacts generation quality from different aspects, further demonstrating its advantages in maintaining geometric consistency and detail fidelity.

Geometric quality of Mesh Head

Figure 6 illustrates the geometric quality of Mesh Head at different initialization steps. Without LPE, the Mesh Head exhibits noticeable unreasonable geometric structures, which persist throughout optimization. In contrast, with LPE, Talk2Me learns more stable and coherent geometric formations, and the rendered images at corresponding steps demonstrate significantly better quality. This indicates that LPE not only enhances positional encoding, but also provides stronger adaptability to finer

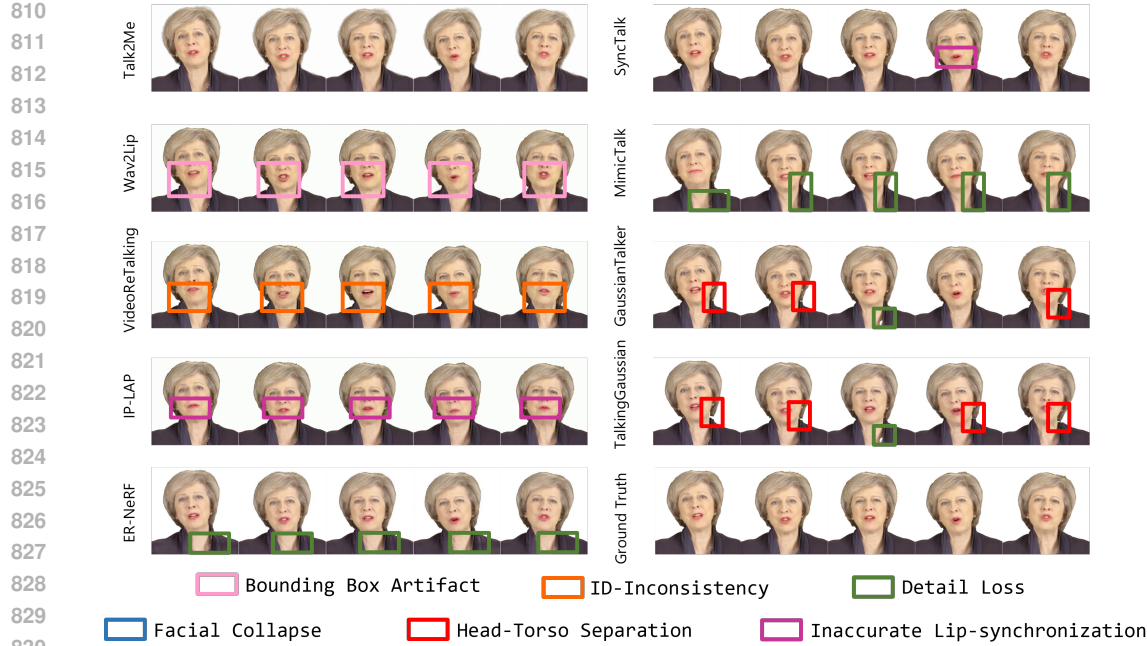


Figure 5: **Qualitative comparison of lip-sync performance on the supplementary dataset (Speaker B).** **Talk2Me** achieves superior lip-sync accuracy and identity preservation, with results close to the ground truth and fewer artifacts compared to prior GAN-, NeRF-, and 3DGS-based methods. Please zoom in for more details.

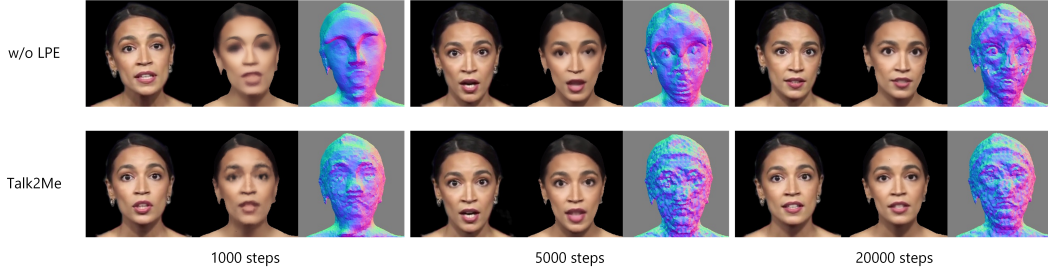


Figure 6: **Visualization of Mesh Head geometry at different training steps with and without LPE.** Without LPE, unreasonable geometric structures persist throughout optimization, while LPE leads to more stable geometry and higher-quality renderings.

local deformations. On top of the general geometric patterns captured by standard PE, LPE performs adaptive optimization, leading to superior structural fitting and more reliable reconstruction quality.

Preservation of Pupil Illumination

To examine the role of LPE in preserving eye illumination, we compare Gaussian Head renderings with and without LPE, as shown in Figure 7. With LPE, Talk2Me better preserves illumination in the eye region, resulting in higher brightness and greater visual fidelity. In contrast, without LPE, the ability to retain illumination details decreases, making the eyes appear darker and less bright, which leads to local detail loss and degraded visual fidelity. These results demonstrate that LPE



884 **Figure 7: Comparison of Gaussian Head renderings with and without LPE.** Without LPE,
885 the ability to preserve illumination details in the eye region decreases, making the overall appearance
886 darker and less bright. In contrast, LPE better maintains eye-region lighting, resulting in brighter
887 and more faithful visual appearance. Please zoom in for detail.



913 **Figure 8: Visualization of eye detail preservation in Gaussian Head renderings.** Without LPE,
914 noticeable artifacts emerge in the eye region during blinking, whereas LPE enables Talk2Me to
915 capture fine-grained dynamics with stable geometry and improved rendering quality.

916
917

918 significantly enhances the model’s ability to capture subtle lighting variations, thereby improving
 919 the realism of the generated results.
 920

921 **Preservation of Eye Details**

922 Furthermore, to evaluate the effectiveness of LPE in detail preservation, we compare Gaussian Head
 923 renderings with and without LPE, as shown in Figure 8. Without LPE, the eye region exhibits
 924 noticeable artifacts, leading to unstable geometry and loss of fine details. In contrast, with LPE,
 925 Talk2Me better captures subtle dynamics such as blinking, maintains stable geometric structures,
 926 and significantly improves overall rendering quality. These results further demonstrate the critical
 927 role of LPE in high-fidelity detail modeling.
 928

929 A.2.3 ABLATION ON TRAINING OBJECTIVES

931 **Table 4: Ablation study on loss terms for Gaussian Avatar training.** **Bold** and underlined indicate
 932 the best and second-best results, respectively.
 933

934 Loss Term	935 PSNR↑	936 LPIPS↓	937 MS-SSIM↑	938 FID↓
L_1	28.867	0.054	0.975	0.218
$L_1 + L_p$	<u>28.658</u>	0.045	0.973	0.113
$L_1 + L_p + L_s$	29.724	0.042	0.977	0.112
$L_1 + L_p + L_s + L_a$	29.966	<u>0.038</u>	0.978	0.014

939 **Table 5: Ablation study on loss terms for RBPG training.** **Bold** and underlined indicate the best
 940 and second-best results, respectively.
 941

942 Loss Term	943 LSE-D↓	944 LSE-C↑
$L_{gan} + L_{vel}$	—	—
$L_{vel} + L_{rec}$	<u>8.282</u>	7.088
$L_{gan} + L_{rec}$	8.254	6.844
$L_{gan} + L_{rec} + L_{vel}$	7.949	7.162

945 To assess the contribution of each loss, we run ablations on **Gaussian Avatar** and **RBPG** (Eq. 10,
 946 Eq. 12); results are reported in Table 4 and Table 5. For Gaussian Avatar, adding the perceptual
 947 loss L_p to L_1 improves perceptual quality: LPIPS changes from 0.054 to 0.045 and FID from
 948 0.218 to 0.113, while PSNR and MS-SSIM decrease slightly. Introducing the SSIM loss L_s then
 949 recovers fidelity, raising PSNR and MS-SSIM to 29.724 and 0.977, and further improving perceptual
 950 metrics (LPIPS = 0.042, FID = 0.112). Finally, adding the adversarial term L_a provides the largest
 951 perceptual gain and the best overall accuracy (PSNR = 29.966, MS-SSIM = 0.978; LPIPS = 0.038,
 952 FID = 0.014).
 953

954 For RBPG, note that removing the reconstruction loss prevents the model from generating plausible
 955 poses, and thus no results are reported in this case. Adding the velocity smoothness loss substantially
 956 improves temporal coherence (reflected by a lower LSE-D), while the adversarial loss enhances
 957 realism and reduces motion artifacts. The full objective achieves the most favorable trade-off, reaching
 958 the lowest LSE-D and highest LSE-C, which demonstrates the necessity of jointly considering all
 959 components.
 960

961 A.3 MODEL ARCHITECTURE AND IMPLEMENTATION

962 In this section, we provide a more detailed description of the proposed **Expression Generator** and
 963 the **Pose Refiner**.
 964

965 EXPRESSION GENERATOR

966 In Figure 9, we present a more detailed processing pipeline inside the **Expression Generator (EG)**.
 967 First, the input audio is processed by *wav2vec* to extract initial audio features. Then, we leverage
 968 a pre-trained *Wav2Lip* model to obtain richer audio representations, which provide more lip-related
 969 information. These audio features are then fed into an *Audio Encoder*, which maps them into the
 970 latent space of expression features. Simultaneously, an *Expression Encoder* extracts facial style
 971 features from a reference frame.
 972

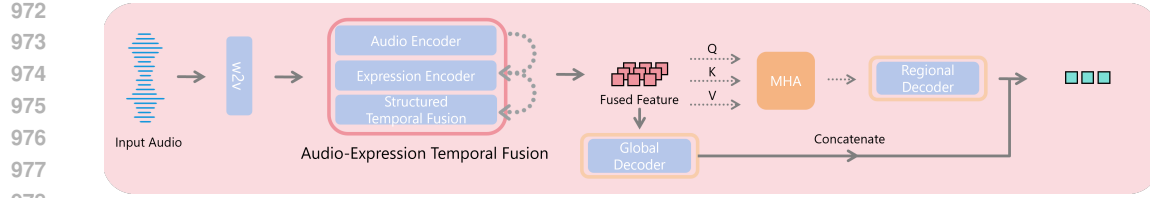


Figure 9: **Architecture of the Expression Generator (EG).** EG fuses audio and visual features via temporal modeling and outputs the predicted expression using both regional and global branches.

Then, a *Structured Temporal Fusion* module performs temporal modeling of the two modalities within the shared latent space, capturing cross-modal temporal correlations and outputting a fused feature representation.

After obtaining the fused feature, we design two branches to jointly predict the final expression. For the **AETF branch**, the fused feature is first processed by a *Multi-Head Attention* layer, followed by a *Regional Decoder* to generate a regional expression feature enriched with localized details. For the global branch, a more straightforward pathway is used to directly predict a *global expression feature* from the fused representation, which carries higher-level phonetic information. Finally, a lightweight, learnable weighting layer combines both branches as input and outputs the *Predicted Expression*.

ENCODER AND DECODER

All the encoders and decoders introduced in EG share the same lightweight architecture, as illustrated in Figure 10. This architecture consists of a few linear layers combined with *ReLU* activation function. Despite its simplicity, the design achieves superior performance while maintaining low computational overhead.

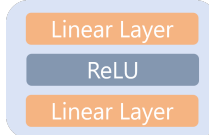


Figure 10: **Shared encoder-decoder architecture used in EG.** A lightweight design combining linear layers and ReLU, achieving efficiency without sacrificing performance.



Figure 11: **STF module for multimodal fusion.** Audio and expression features are fused via gating, K-product interaction, and a Transformer layer to enhance temporal modeling.

STRUCTURED TEMPORAL FUSION.

The **STF** module within EG is illustrated in Figure 11. The features obtained from the *Audio Encoder* and *Expression Encoder* are first processed by a *feature gate* and a *K-product fusion* module, resulting in *Embedding G* and *Embedding K*, respectively. These embeddings are then fed into a *Transformer Layer*, which effectively aggregates expression and audio features, thereby enriching the temporal correlation information within the generated fused feature.

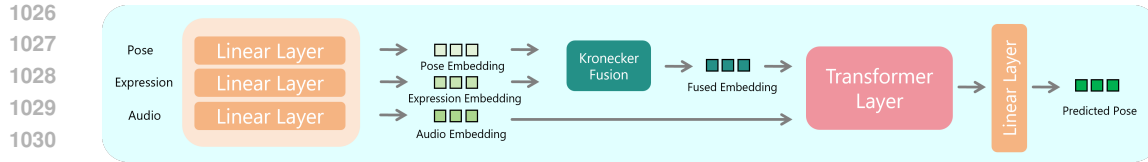


Figure 12: **Pose Refiner (PR)**. Architecture of the PR module in RBPG. Pose, expression, and audio features are projected via linear layers. Pose and expression embeddings are fused using Kronecker Fusion, then combined with the audio embedding and processed by a Transformer layer. A final linear layer outputs the predicted pose.

POSE REFINER

The architecture of the **Pose Refiner** within the **Retrieval-Based Pose Generator (RBPG)** is shown in Figure 12. The retrieved pose, expression feature, and audio feature are each passed through individual linear layers to be projected into a shared latent space. Subsequently, a *Kronecker Fusion* layer takes the *pose embedding* and *expression embedding* as input to further model the relationship between facial expression and head pose. After this operation, the resulting *fused embedding*, along with the *audio embedding*, is fed into a *Transformer Layer*. The output is then passed through a final linear layer to produce smooth and natural head poses.

A.4 USER STUDY DESIGN AND QUESTIONNAIRE

A.4.1 OVERVIEW

To assess the perceptual quality of the generated talking head videos, we conduct a user study to evaluate the perceptual quality of the generated talking head videos following the standard Mean Opinion Score (MOS) protocol. The evaluation focuses on five key aspects:

- **Lip-sync accuracy (Lip):** Alignment between lip movements and spoken audio.
- **Expression synchronization (Exp):** Temporal and semantic consistency between facial expressions and the speech content.
- **Pose synchronization (Pose):** Naturalness and coherence of head movement in response to speech.
- **Image quality (Img):** Visual fidelity, clarity, and absence of artifacts.
- **Video realness (Vid):** Overall realism of the video, including identity consistency and expressiveness.

Each criterion is rated on a 5-point Likert scale, where 1 indicates "poor" and 5 indicates "excellent." Participants watch anonymized video clips generated by various methods, including GAN-based, NeRF-based, 3DGS-based baselines, and our proposed **Talk2Me** model.

A.4.2 STUDY SETUP

We conduct an anonymous online survey and obtain 120 valid responses. Each participant views a randomized set of anonymized video clips, each lasting 30–60 seconds, to reduce ordering effects and bias. Participants are asked to watch and rate the videos according to five specific criteria. They may replay each video as many times as needed before submitting their responses. No time limits are imposed, and participants complete the questionnaire at their own convenience.

The video dataset comprises a diverse set of speakers and utterances to mitigate potential bias related to speaker identity or language content. All participants are bilingual in English and Chinese.

1080 A 4.3 ETHICS AND CONSENT

1081

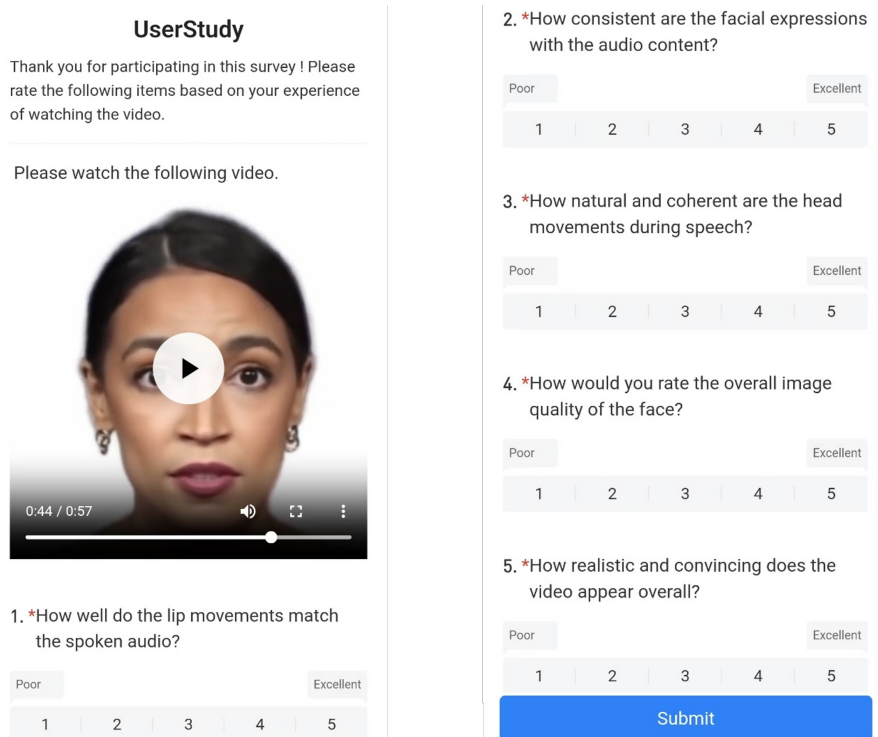
1082 All participants provide informed consent before participating in the study. They are informed about
1083 the purpose of the study, data privacy protection, and their right to withdraw at any time without
1084 consequence. No personal or identifiable data is collected.

1085 The study involves non-sensitive, anonymous video content, while adhering to standard ethical
1086 guidelines for human-subject research.

1087

1088 A.4.4 QUESTIONNAIRE

1089



1114 **Figure 13: User Study Questionnaire.** Participants rate generated videos on five aspects using a 5-
1115 point Likert scale: lip-sync accuracy (Lip), expression synchronization (Exp), pose synchronization
1116 (Pose), image quality (Img), and video realness (Vid).

As shown in Figure 13, each participant answers the following five questions after watching each video clip:

1. How well do the lip movements match the spoken audio? (**Lip-sync accuracy**)
2. How consistent are the facial expressions with the audio content? (**Expression synchronization**)
3. How natural and coherent are the head movements during speech? (**Pose synchronization**)
4. How would you rate the overall image quality of the face? (**Image quality**)
5. How realistic and convincing does the video appear overall? (**Video realism**)

1127 All responses are collected digitally, and we compute the average MOS scores for each method and
1128 evaluation criterion. The final results are summarized in Table 2, where the best and second-best
1129 scores are shown in bold and underlined, respectively.

1130

A.4.5 ANALYSIS AND RESULTS

1132

As shown in Table 2, **Talk2Me** achieves the highest scores in four out of five evaluation aspects, and outperforms recent GAN-, NeRF-, and 3DGS-based methods. The method shows clear advantages

1134 in audiovisual coherence and expressiveness. Although it ranks slightly lower in raw image quality,
1135 it demonstrates balanced and robust performance overall, generating high-fidelity and controllable
1136 facial animation that remains well synchronized with the input audio.
1137

1138 A.5 LARGE LANGUAGE MODEL USAGE

1139
1140 In the process of writing this paper, we use a large language model (LLM) solely to refine the
1141 phrasing and improve the clarity of the text. The LLM is not involved in the design of the method,
1142 the experiments, or the analysis of results.
1143

1144 A.6 REPRODUCIBILITY

1145 We ensure reproducibility by providing clear distinctions between results and interpretations, and
1146 by reporting implementation details such as hyperparameters, evaluation metrics, and computing
1147 infrastructure. All external datasets used in this work are publicly available and properly cited. In
1148 addition, we construct a small Chinese dataset, which will also be released upon publication. While
1149 certain aspects such as random seed settings and statistical significance tests are not reported, the
1150 information and resources provided are sufficient to enable independent reproduction of our results.
1151

1152 A.7 ETHICAL CONSIDERATIONS IN AVATAR GENERATION

1153
1154 Our proposed method can be applied to avatar generation, enabling more realistic and stable 3D
1155 reconstructions. While such technology has promising applications in areas like virtual communica-
1156 tion and entertainment, it may also raise concerns if misused. We therefore call for the responsible
1157 and ethical use of this technology to ensure it benefits creative and human-centered applications
1158 without infringing on privacy or identity rights.
1159
1160
1161
1162
1163
1164
1165
1166
1167
1168
1169
1170
1171
1172
1173
1174
1175
1176
1177
1178
1179
1180
1181
1182
1183
1184
1185
1186
1187